

# The Tetragonal Deformation of the $\text{TiO}_6$ Octahedron in Ferroelectric $\text{PbTiO}_3$

J. G. BERGMAN, G. R. CRANE, AND E. H. TURNER

*Bell Laboratories, Holmdel, New Jersey 07733*

Received December 8, 1976

The  $9^\circ$  tetragonal deformation of the  $\text{TiO}_6$  octahedron in  $\text{PbTiO}_3$  is monitored as a function of temperature by employing a three-dimensional bond polarizability model to analyze the temperature dependence of optical second harmonic generation (SHG). The utility of monitoring crystal phase transitions in this manner is further demonstrated by combining the results of this analysis with previously published pyroelectric measurements to find the spontaneous polarization of this material.

## Introduction

It has recently been shown (1) that by using a three-dimensional polarizability model to analyze the temperature dependence of bulk second harmonic generation (SHG) coefficients, one can obtain detailed information on a microscopic scale regarding the nature of solid-state phase transitions. The technique has now been used successfully to describe tetrahedral rotations (2, 3) ( $\text{SiO}_4$ ,  $\text{GeO}_4$ ) as well as trigonal (4) and tetragonal (5) deformations of octahedra. Such a model is applied here to describe the large ( $9^\circ$ ) tetragonal deformation of the  $\text{TiO}_6$  octahedron in  $\text{PbTiO}_3$  as a function of temperature. The same tetragonal deformation model is also applied to the temperature dependent spontaneous polarization, with quite good results.

The essence of the theory is the simple coordinate transformation relation

$$d_{ijk} = \frac{1}{V} G_{il} G_{jm} G_{kn} \beta_{lmn}, \quad (1)$$

where the  $3 \times 3$  transformation matrix of direction cosines ( $G$ ) takes the microscopic bond polarizability  $\beta$  (bond coordinate system), into the macroscopic crystal polarizability  $d$  (crystal coordinate system), the scale factor  $V$  being the volume of the unit cell. Since  $G$  is an orthonormal matrix its nine

general elements can be expressed in terms of the three independent elements ( $l, m, n$ ) which are the direction cosines of the bond with respect to the crystal ( $x, y, z$ ) axes, respectively. Furthermore, since many nonlinear coefficients ( $d_{333}$  for example) involve only one direction cosine ( $n \equiv \cos\phi_z$ ) one can readily express  $d$  as a function of one angle  $\phi$ :

$$d_{333} = \sum_s \beta^s f^s(\phi_z). \quad (2)$$

Our approach to investigate a phase transition is to assume that the major change in  $d(\text{obs})$  vs temperature is due to a change in some bond angle rather than a change in  $\beta$ , viz.,

$$\partial f(\phi)/\partial T \gg \partial \beta/\partial T, \quad (3)$$

thus simplifying Eq. (2) to

$$d_{333} = kf(\phi_z). \quad (4)$$

This assumption (Eq. (3)) has been shown to be valid in the several cases thus far investigated (1-5). In other words, one uses the temperature dependence of  $d$  to monitor the temperature dependence of some bond angle  $\phi$  in a crystal.

The basic relation, Eq. (1), is exactly analogous to that used for many years (6) to determine linear bond polarizabilities  $\alpha$ 's,

$$\chi_{ij} = \frac{1}{V} G_{il} G_{jm} \alpha_{lm}. \quad (5)$$

A major difficulty with using Eq. (5) for studying phase transitions is that  $\chi$ 's seldom change by more than a few percent. On the other hand,  $d$ 's often change by over an order of magnitude. Our microscopic model for a bond hyperpolarizability  $\beta$  is also exactly analogous to that used previously (6) for the linear bond polarizability  $\alpha$ , where the bond has cylindrical symmetry ( $C_{\infty v}$ )

$$\alpha_{ij} = \begin{pmatrix} \alpha^\perp & 0 & 0 \\ 0 & \alpha^\perp & 0 \\ 0 & 0 & \alpha^\parallel \end{pmatrix}, \quad (6)$$

having  $\alpha^\perp \equiv \alpha_{11} = \alpha_{22}$  and  $\alpha^\parallel \equiv \alpha_{33}$ . Similarly,

$$\beta_{ijk} = \begin{pmatrix} 0 & 0 & 0 & 0 & \beta^\perp & 0 \\ 0 & 0 & 0 & \beta^\perp & 0 & 0 \\ \beta^\perp & \beta^\perp & \beta^\parallel & 0 & 0 & 0 \end{pmatrix}, \quad (7)$$

where  $\beta^\perp \equiv \beta_{311} = \beta_{322} = \beta_{223} = \beta_{232} = \beta_{113} = \beta_{131}$  and  $\beta^\parallel \equiv \beta_{333}$ . Thus using  $d_{333}$ , for example, and Eq. (1) one finds

$$d_{333} = \frac{1}{V} \sum_i n_i^3 \beta_i^\parallel + 3n_i(1 - n_i^2) \beta_i^\perp, \quad (8)$$

where the  $i$ th bond has a polarizability (7) ( $\beta^\parallel, \beta^\perp$ ) <sub>$i$</sub>  and makes an angle  $\phi_i$  ( $n_i = \cos \phi_i$ ) with the crystal  $z$  axis. Likewise for  $d_{311}$  we find

$$d_{311} = \frac{1}{V} \sum_i l_i^2 n_i \beta_i^\parallel + n_i(1 - 3l_i^2) \beta_i^\perp, \quad (9)$$

where  $l_i$  and  $n_i$  are the respective direction cosines of the  $i$ th bond with respect to the crystal  $x$  and  $z$  axes. The functional form of the only other allowed coefficient in  $4mm$  symmetry ( $d_{131}$ ) is identical to that of  $d_{311}$  (Eq. 9), and Kleinman has shown (8) that in the absence of dispersion,  $d_{311} = d_{131}$ . This result has also been verified experimentally by Singh, Remeika, and Potopowicz (9) for  $\text{PbTiO}_3$ .

The well-characterized structure (10) of the centric ( $m3m$ ) high-temperature ( $T > T_c \sim 120^\circ\text{C}$ ) phase of the isomorphous prototype ferroelectric  $\text{BaTiO}_3$  is shown in Fig. 1 where we see the 12 coordinate Ba atoms at the center of the cube and the six coordinate titanium atoms at the cube corners, the oxygen atoms

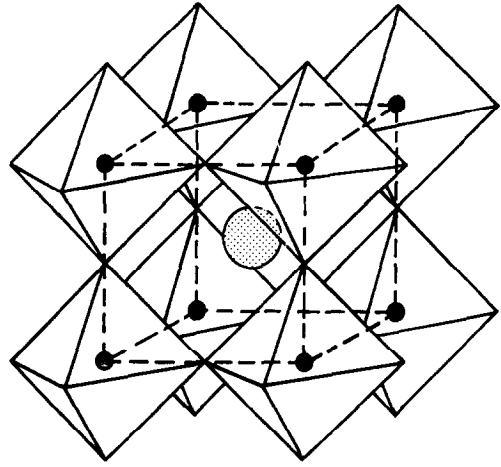


FIG. 1. Structure of  $\text{BaTiO}_3$  and  $\text{PbTiO}_3$  in their centric ( $m3m$ ) high temperature phases, showing the 12 coordinate Ba (Pb) atom at the center of the cube and the six coordinate Ti atoms at the cube corners, the oxygens being situated at the midpoints of the cube edges.

being situated at the midpoints of the cube edges. In the acentric  $4mm$  (polar) room temperature (10) phase (Fig. 2) the oxygens have moved down by  $\delta\phi = 3^\circ$  ( $\phi = 93^\circ$ ) causing a 1.5% change in the Ba-O bond lengths.

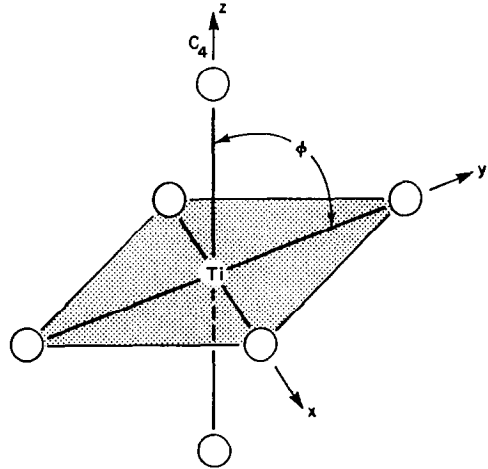


FIG. 2. Octahedral distribution of oxygens about Ti in  $\text{PbTiO}_3$  showing the fourfold axis ( $C_4$ ) and the deformation angle  $\phi$ . The range of  $\phi$  is from  $98.6^\circ$  at room temperature to  $90^\circ\text{C}$  at  $T \geq T_c = 490^\circ\text{C}$ .

The structure of the high-temperature phase ( $T > T_c \sim 490^\circ\text{C}$ ) for PbTiO<sub>3</sub> is basically the same as that of BaTiO<sub>3</sub> (Fig. 1). Hence the lone pair of valence electrons on the Pb can be thought of as occupying the centric 6S level. However, in the room temperature structure (11) (Fig. 2) it is found that the oxygens have moved down by  $\delta\phi \sim 9^\circ$  ( $\phi = 98.6^\circ$ ) causing a 11.5% change in the Pb–O bond lengths. Thus if one uses this bond length anisotropy ( $d_{\text{long}} - d_{\text{short}}/\langle d \rangle$ ) to describe the Ba and Pb environments one finds that the Pb environment is almost an order of magnitude more anisotropic than the Ba environment, i.e., (25 vs 3%). This distortion, which is larger than one might expect, can be thought of as arising from the lone pair of electrons on the Pb atom, i.e., as the top four oxygens (Fig. 1) get closer to the lead and become more covalent the lead orbitals become rehybridized as some of the 6S level is used for the bonding interaction. In fact, the lead environment, as noted by Megaw (12), is remarkably similar to that found in lead oxide where the four oxygens are situated at the corners of a square pyramid with the stereochemically active lone pair at the apex giving an  $sp^3d$  hybrid (13). Thus the degree to which the lone pair in PbTiO<sub>3</sub> is involved in bonding (its stereochemical activity) is proportional to the proximity of the top (short) set of oxygens. This situation is quite similar to that found in the iodates where one has an  $sp^3$  hybridized iodine which contains three close oxygens and a stereochemically active lone pair. Because of the increased stereochemical activity of the lead lone pair, we must include polarizability contributions from the lead–oxygen bonding. By analogy with the approximation used in the iodate structures (14, 15), we use an  $sp^3d$  hybrid (in this case, an inverted square pyramid with four oxygens at the top and a lone pair at the bottom) and where  $\beta_{\text{LP}} \sim \beta_{\text{Pb-O}}$ . Using this model of the lead environment, and the octahedral Ti–O distribution we find from Eqs. (8) and (9) and the structural data (11) that

$$d_{333} = \frac{1}{V}(-0.013\beta_{\text{Ti}}^{\parallel} - 1.753\beta_{\text{Ti}}^{\perp} + 0.030\beta_{\text{Pb}}^{\parallel} + 4.544\beta_{\text{Pb}}^{\perp}). \quad (10)$$

$$d_{311} = \frac{1}{V}(-0.292\beta_{\text{Ti}}^{\parallel} + 0.278\beta_{\text{Ti}}^{\perp} + 0.757\beta_{\text{Pb}}^{\parallel} - 0.727\beta_{\text{Pb}}^{\perp}). \quad (11)$$

Using the  $(\beta^{\parallel}, \beta^{\perp})_{\text{Ti}}$  values found previously (5) from BaTiO<sub>3</sub> of  $(35.5, 2.2) \times 10^{-30}$  esu and the nonlinear coefficients  $(d_{333}, d_{311})$  for PbTiO<sub>3</sub> of  $(+20, -97) \times 10^{-9}$  esu (9, 16) we find from Eqs. (10, 11)  $(\beta^{\parallel}, \beta^{\perp})_{\text{Pb}}$  to be  $(5.7, 1.2) \times 10^{-30}$  esu. For consistency we have set up our BaTiO<sub>3</sub> absolute configuration with the same polarity as PbTiO<sub>3</sub> so that with  $(d_{333}, d_{311})$  for BaTiO<sub>3</sub> of  $(-21, -54) \times 10^{-9}$  esu we find  $(\beta^{\parallel}, \beta^{\perp})_{\text{Ti}}$  to be  $(+35.5, 2.2) \times 10^{-30}$  esu. It is worth noting that the change in sign of  $d_{333}$  (PbTiO<sub>3</sub>) relative to  $d_{333}$ (BaTiO<sub>3</sub>) is caused by the small  $\beta_{\text{Pb}}^{\perp}$  term and its large geometrical factor. Thus we can conclude from Eq. (10) that if we had used a one-dimensional model ( $\beta^{\perp} = 0$ ) we would have lost the largest terms  $(\beta_{\text{Ti}}^{\perp}, \beta_{\text{Pb}}^{\perp})$  in  $d_{333}$ . In agreement with microscopic theories (17, 18) we find  $\beta^{\parallel} \gg \beta^{\perp}$  ( $\beta_{\text{Ti}}^{\parallel} = 16\beta_{\text{Ti}}^{\perp}$ ;  $\beta_{\text{Pb}}^{\parallel} = 5\beta_{\text{Pb}}^{\perp}$ ). Again, because of the importance of geometrical factors one is not justified in general in neglecting  $\beta^{\perp}$ .

Following Levine's suggestion, (19) we have attempted to replace this phenomenological method of obtaining  $\beta$ 's with his Bond Charge Theory (20), a one-dimensional theory, i.e., ( $\beta^{\perp} \equiv 0$ ). While this calculation gives a reasonable account of the magnitude and sign of the individual bond nonlinearities ( $\beta^{\parallel}$ 's), the total nonlinear susceptibility, however, is not in agreement with experiment viz  $d_{333}^{\text{cal}} = +6.4 \times 10^{-30}$  esu,  $d_{333}^{\text{obs}} = -20 \times 10^{-30}$  esu. Levine has pointed out (21), however, that this due to an accidental near cancellation between the various bonds for the particular case of PbTiO<sub>3</sub>.

In order to describe the temperature dependence of the observed  $d$ 's in terms of a microscopic model we recall (Fig. 1) that the Pb–O bonds are directly coupled to the Ti–O bonds since they are both (Pb, Ti) bonded to the same oxygens. Hence as the crystal cools down from  $T > T_c \sim 490^\circ\text{C}$ , the Pb environment should deform at the same rate as the Ti environment. Since the nonlinear coefficients depend directly on this temperature dependent deformation (change in  $\phi$ ) the temperature

dependence of the Pb and Ti contributions must be the same. For simplicity then we take

$$d_{333}(T) \propto \frac{1}{V} (35.5 \cos^3 \phi(T) + 6.6 \cos \phi(T) \sin^2 \phi(T)). \quad (12)$$

$$d_{311}(T) \propto \frac{1}{V} [35.5 \cos \phi(T) \sin^2 \phi(T) - 2.2 \cos \phi(T) (2-3 \cos^2 \phi(T))], \quad (13)$$

where 35.5 and 6.6 are  $\beta_{Ti}^{\parallel}$  and  $\beta_{Ti}^{\perp}$ , respectively. Thus using our room temperature conditions,  $\phi = 98.6^\circ$  and  $(d_{333}, d_{311}) = (+20, -97) \times 10^{-9}$  esu and Eqs. (12 and 13) we find

$$d_{333} = (-122 \times 10^{-9} \text{ esu}) (5.4 \cos^3 \phi + \cos \phi \sin^2 \phi). \quad (14)$$

$$d_{311} = (46.8 \times 10^{-9} \text{ esu}) [16.1 \cos \phi \sin^2 \phi - \cos \phi (2-3 \cos^2 \phi)]. \quad (15)$$

Thus we now have a direct relation between a measurable coefficient  $d_{333}$  and/or  $d_{311}$  and the angle  $\phi$  between the Ti-O bond and the crystal  $z$  axis, so that we can monitor  $\phi$  as a function of temperature by following  $d$  vs  $T$ .

A schematic representation of the experimental apparatus is given in Fig. 3. Details

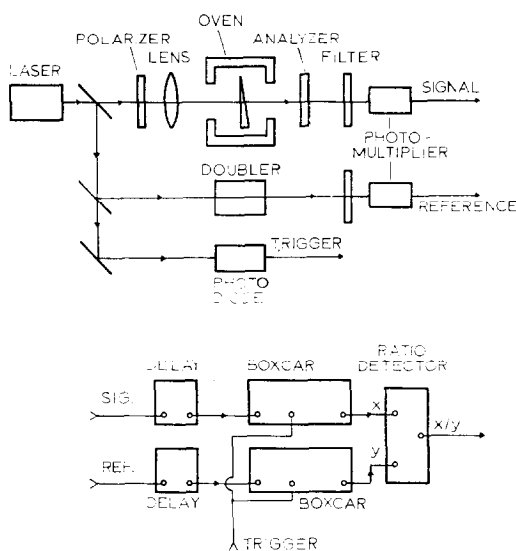


FIG. 3. Schematic of experimental setup used to measure the temperature dependence of the nonlinear coefficients in  $\text{PbTiO}_3$ .

of the experimental procedure are given elsewhere (14), but a brief discussion of the method follows. Figure 4 shows a typical plot of the observed second harmonic intensity ( $I^{2\omega}$ ) versus the translation distance ( $D$ ) of our wedge, the wedge being translated perpendicular to the propagation direction of our  $1.06\text{-}\mu$  beam. The wedge angle  $\theta$  varied from  $1^\circ$  to  $5^\circ$  on the several samples. The coherence length  $l_c$  is related to the wedge angle  $\theta$  and the translation distance  $D$  via

$$l_c = \frac{1}{2} D \tan \theta. \quad (16)$$

Hence from such a plot (Fig. 4) one can readily determine both the intensity ( $I^{2\omega}$ ) as well as the coherence length  $l_c$  for any one particular temperature, the relation between these two parameters ( $l_c, I^{2\omega}$ ) and the nonlinear coefficient  $d$  being

$$d \propto \frac{1}{l_c} (I^{2\omega})^{1/2}. \quad (17)$$

Thus from a series of plots such as Fig. 4

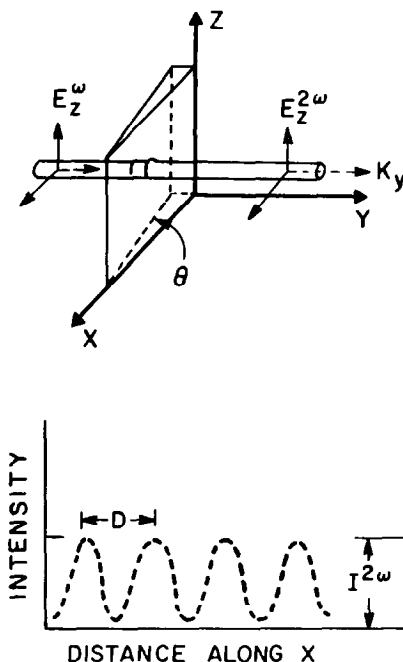


FIG. 4. Typical plot of observed second harmonic intensity  $I^{2\omega}$  versus wedge translational distance  $D$  showing the detail of the crystal coordinate system, the wedge configuration and the laser propagation direction  $K$ .

at a series of temperatures one determines the temperature dependence of  $d$ . Corrections for reflection losses (14) were neglected since the refractive indices are almost isotropic. Our experimental results are shown in Fig. 5. Using Eqs. 14 and 15, we find the temperature dependence of  $\phi$  to be that shown in Fig. 6. Since the temperature dependence of the  $d$ 's was a well-behaved function whose observed spread was  $\sim 5\%$ , we thus assume the uncertainty in  $\phi$  to also be  $\sim 5\%$ .

We were unable to obtain a direct confirmation of Miller and Nordland's (16) sign relation ( $d_{333} \times d_{311} < 0$ ) using the wedge technique and a  $\frac{1}{4}$  wave plate (22), because of the accidental degeneracy of the two coherence lengths ( $l_{33} \cong l_{31}$ ) and the limited length of our wedge. Suffice it to say, however, that the intensities of the two interference signals were completely consistent with the earlier room temperature sign determination (23) via the Maker technique (24).

We have also measured the Pockels or linear electrooptic effect and find that the appropriate  $d$  coefficients,  $d_{311}^{\text{eo}}$  and  $d_{333}^{\text{eo}}$ , have the same sign. These coefficients include lattice contributions due to optical phonons in addition to the purely electronic SHG components. Our results (25) for ( $d_{333}^{\text{eo}}, d_{311}^{\text{eo}}$ ) are  $(-170, -380) \times 10^{-9}$  esu, where the signs

are related to the spontaneous polarization direction, i.e., consistent with the nonlinear optical (SHG) signs. These magnitudes are much larger than the SHG values for ( $d_{333}, d_{311}$ ) so the lattice contributions are dominant. However, it is of interest that  $|d_{311}^{\text{eo}}| > |d_{333}^{\text{eo}}|$  whereas in other ferroelectrics this inequality is reversed (25, 26). This is consistent with the positive sign for  $d_{333}$  found by Miller and Nordland (16) since that reduces the magnitude of  $d_{333}^{\text{eo}}$ , whereas in other ferroelectrics the lattice and SHG portions have the same sign.

## Discussion

It is interesting to note that the analysis and measurements of the preceding section can be combined with the pyroelectric measurements of Remeika and Glass (17) to find the spontaneous polarization  $P_s$  for PbTiO<sub>3</sub>. Specifically, if  $\phi = 90^\circ$  is the measure of crystal anisotropy it follows that the spontaneous polarization  $P_s$  is given by

$$P_s = k \cos \phi. \quad (20)$$

A least-squares fit of the pyroelectric data (27) and Eq. (20) using SHG determined angles  $\phi_i(T)$  yields a constant  $k$  of  $522.0 \mu\text{C}/\text{cm}^2$  and a room temperature spontaneous polarization  $P_s$  of  $82.3 \mu\text{C}/\text{cm}^2$  which compares favorably with the recent experimental value of  $75 \mu\text{C}/\text{cm}^2$  estimated by Carl (28) as well as with the value of  $80 \mu\text{C}/\text{cm}^2$  which is obtained by setting  $P_s$  proportional to the square root of the spontaneous strain (10), i.e.,

$$P_s \propto (1 - c/a)^{1/2} \quad (21)$$

and then using the tabulated values (10) of  $c/a$  and the pyroelectric measurements to find  $P_s$ .

It is also worth noting that if we assume a bond additivity model for  $P_s$  analogous to Eq. (1),

$$P_i = \frac{1}{V} \sum G_{ij} \mu_j, \quad (22)$$

then the contribution of the Ti  $\rightarrow$  O bonds is given by

$$P = \frac{4\mu}{V} \cos \phi. \quad (23)$$

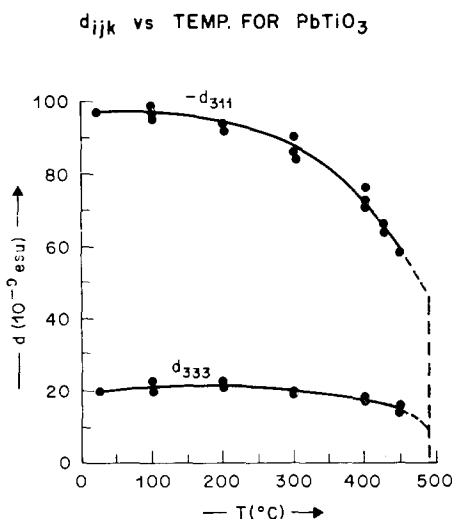


FIG. 5. Observed temperature dependence of the nonlinear coefficients  $d_{333}$  and  $d_{311}$  for PbTiO<sub>3</sub>.

so that if we use the result  $\mu(\text{Ti} \rightarrow \text{O}) = 24$  Debye, obtained (5) from  $\text{BaTiO}_3$  we would obtain  $P_s(\text{Ti} \rightarrow \text{O}) = 76 \mu\text{C}/\text{cm}^2$  at room temperature, which implies that the  $\text{Pb} \rightarrow \text{O}$  contribution to  $P_s$  is very small.

As a final test of self-consistency, we may use the adjusted pyroelectric measurements of Fig. 7 with  $k = 522 \mu\text{C}/\text{cm}^2$  in Eq. (20) to give values of  $\phi(T)$ . These are shown in Fig. 6 to agree well with the SHG determined angles.

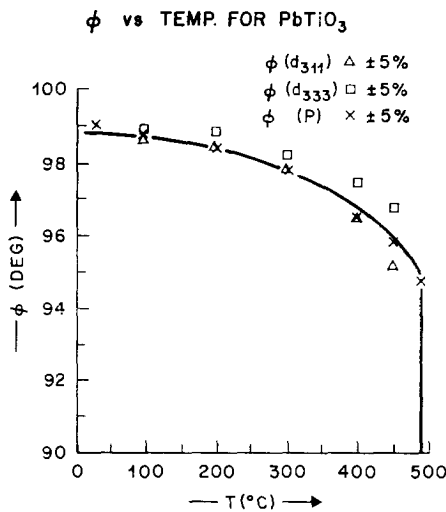


FIG. 6. Temperature dependence of the tetragonal deformation angle  $\phi$  of the  $\text{TiO}_6$  octahedron (Fig. 2) in  $\text{PbTiO}_3$  as determined from  $d_{333}(\phi)$ ,  $d_{311}(\phi)$  and  $P(\phi)$ .

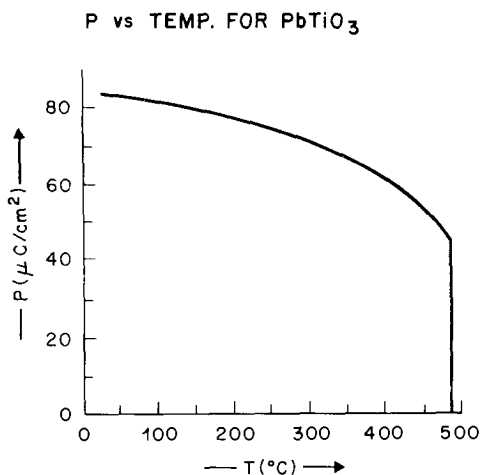


FIG. 7. Temperature dependence of the spontaneous polarization  $P$  for  $\text{PbTiO}_3$ .

In summary we have shown that by using a primitive additivity model for both the spontaneous polarization and the nonlinear coefficients one can obtain detailed information on a microscopic scale regarding the nature of the solid state phase transition in  $\text{PbTiO}_3$ .

### Acknowledgments

We would like to thank R. C. Miller for supplying the  $\text{PbTiO}_3$  crystal and B. F. Levine for aid in the bond charge calculation.

### References

1. J. G. BERGMAN, *Chem. Phys. Lett.* **38**, 230 (1976).
2. J. G. BERGMAN AND G. R. CRANE, *Chem. Phys. Lett.* **4**, 133 (1976).
3. G. R. CRANE AND J. G. BERGMAN, *J. Appl. Cryst.* **9**, 476 (1976).
4. J. G. BERGMAN, *J. Amer. Chem. Soc.* **98**, 1054 (1976).
5. J. G. BERGMAN, *Inorganic Chem.* **15**, 1743 (1976).
6. C. W. BUNN, "Chemical Crystallography," Oxford Press, New York (1961).
7. Since we have neglected the local field effects, it might be more precise to think of  $\beta$  as an "effective" polarizability.
8. D. A. KLEINMAN, *Phys. Rev.* **126**, 1977 (1962).
9. S. SINGH, in "Handbook of Lasers," (R. C. Weast, Ed.), p. 500, Chemical Rubber Co., Cleveland, Ohio (1971).
10. F. JONA AND G. SHIRANE, "Ferroelectric Crystals," Pergamon Press, New York (1962).
11. G. SHIRANE, R. PEPINSKY, AND B. C. FRAZER, *Acta Crystallogr.* **9**, 131 (1956).
12. H. D. MEGAW, *Acta Crystallogr.* **7**, 187 (1954).
13. W. J. MOORE AND L. PAULING, *J. Amer. Chem. Soc.* **63**, 1392 (1941).
14. J. G. BERGMAN AND G. R. CRANE, *J. Chem. Phys.* **60**, 2470 (1974).
15. B. C. TOFIELD, G. R. CRANE, AND J. G. BERGMAN, *J. Chem. Soc. Faraday Trans. II* **70**, 1488 (1974).
16. R. C. MILLER AND W. A. NORDLAND, *Phys. Rev. B* **5**, 4931 (1972).
17. J. M. O'HARE AND R. P. HURST, *J. Chem. Phys.* **46**, 2356 (1967).
18. C. FLYTZANIS AND J. DUCUING, *Phys. Rev.* **178**, 1218 (1969).
19. B. F. LEVINE, *Phys. Rev. B* **13**, 5102 (1976).
20. B. F. LEVINE, *Phys. Rev. B* **10**, 1655 (1974), and references therein.

21. B. F. LEVINE, private communication.
22. G. R. CRANE, *J. Appl. Phys.* **44**, 915 (1973).
23. R. C. MILLER AND W. A. NORDLAND, *Appl. Phys. Lett.* **16**, 174 (1970).
24. P. D. MAKER, R. W. TERHUNE, M. NISENOFF, AND C. M. SAVAGE, *Phys. Rev. Lett.* **8** 21 (1962).
25. I. P. KAMINOW AND E. H. TURNER, in "Handbook of Lasers," Chemical Rubber Co., Cleveland, Ohio (1971). The value of  $d^{60}$  given in this paper corresponds to  $r_{33} = +5.6 \times 10^{-12}$  m/V and  $r_{13} = +12.6 \times 10^{-12}$  m/V. The sign determination is new and the magnitudes differ by a small amount from earlier results in this reference.
26. G. D. BOYD, T. J. BRIDGES, M. A. POLLACK, AND E. H. TURNER, *Phys. Rev. Lett.* **26**, 387 (1971).
27. J. P. REMEIKA AND A. M. GLASS, *Mat. Res. Bull.* **5**, 37 (1970).
28. K. CARL, *Ferroelectrics* **9**, 23 (1975).